



Influence of Wax Lubrication on Cutting Performance of Single-Crystal Silicon in Ultraprecision Microgrooving

Seyed Nader Ameli Kalkhoran^{1,2} · Mehrdad Vahdati¹ · Zhiyu Zhang³ · Jiwang Yan²

Received: 14 September 2019 / Revised: 18 December 2019 / Accepted: 23 January 2020
© Korean Society for Precision Engineering 2020

Abstract

Lubrication can improve the tool-workpiece interface condition in ultraprecision machining, especially in microgrooving processes. The aim of this study was to compare the effects of dry, liquid (cutting oil), solid (wax) and hybrid (cutting oil and wax) lubrication conditions, on the creation of arc-sectioned microgrooves on single-crystal silicon wafers using a single-crystal diamond tool. Micro cutting forces, chip morphology, and surface quality at different locations of the grooves were investigated. Rose-shaped continuous chips were observed in dry cutting, indicating stable ductile mode material removal. The entrance side of the groove was always smoother than the exit side with a higher degree of phase transformation. Chip adhesions on the tool edge were found in dry and oil lubricated cutting, whereas wax coating could prevent the adhesion. Wax coating played the dual roles of a chip breaker as well as a high-performance lubricant, thus improved the surface integrity. This study demonstrated the capability of using wax coating as an environmentally friendly solid lubricant for microgrooving of single-crystal silicon and possibly for other hard brittle materials.

Keywords Diamond turning · Micro cutting · Ultraprecision machining · Micro groove · Single crystalline silicon · Solid lubricant · Green manufacturing

1 Introduction

In today's industry, the demand for semiconductor components with a highly accurate surface is increasing. Single-crystal silicon is a major semiconductor material for optoelectronic and microelectronics, micro-electro-mechanical systems (MEMS), and solar panels owing to its excellent properties such as high purity, hardness and wear resistance, low thermal expansion, superb stability, light weight, low oxide formability, and abundance. Ultraprecision machining is needed for achieving a mirror-like surface on silicon [1–3].

Surface integrity is a characteristic expression of surface quality including surface roughness, waviness, surface/sub-surface defects and metallurgical changes after a manufacturing process [4, 5]. In ultraprecision machining processes, the ultimate surface integrity may be influenced by various machining parameters, such as depth of cut, tool feed rate, and tool geometry. Any minute changes in these parameters can result in a noticeable discrepancy in the form accuracy and surface roughness [6–8]. In contrast, the effects of lubricants on the ultraprecision machining processes of silicon have not been fully elucidated.

Lubrication can reduce heat generation, and as a result, diminish the cutting temperature [9]. Moreover, an appropriate lubricant may decrease the cutting forces by reducing the friction in the tool-workpiece interface [10]. The use of cutting oil can suppress chip adhesion and tool wear [11]. Conventionally, liquid lubricants such as water and kerosene are used in machining processes of metals [12, 13]. On average, over 36 million metric tons of lubricants are being produced and used per annum in the world; that way, the estimated annually turnover in the US alone is more than 19 billion dollars [14]. Most of these lubricants are liquid and it is estimated that up to 80% of them are released into the

✉ Jiwang Yan
yan@mech.keio.ac.jp

¹ Department of Mechanical Engineering, K.N. Toosi University of Technology, Pardis St., Vanak Sq., Tehran, Iran

² Department of Mechanical Engineering, Keio University, Hiyoshi 3-14-1, Kohoku-ku, Yokohama 223-8522, Japan

³ Key Laboratory of Optical System Advanced Manufacturing Technology, Changchun Institute of Optics, Fine Mechanics and Physics, Chinese Academy of Sciences, Changchun 130033, China

environment [15]. Therefore, a major issue in this area is the prevention of widespread ecological pollution.

Danyluk and Reaves [16] utilized three fluids in the grooving of silicon under a constant thrust force and showed that the deepest and the shallowest grooves were achieved by using acetone and water respectively. Moriwaki et al. [17] used kerosene as the cutting oil in two forms of oil mist and oil jet. They displayed that both conditions lead to a reduction in the temperature rise and machining error. However, using the oil mist was more influential. Yan et al. [18] investigated the effect of kerosene mist and water on the ultraprecision machining of silicon and illustrated that the use of fluids of high cooling ability led to lower ductile machinability, although prolonged the tool life. Liquid lubricants also lowered the ductile machinability of other brittle materials [18–20]. Ohta et al. [21] compared the effect of oil-based and water-based coolants on tool wear in the ultraprecision machining of silicon and elucidated that water-based electrically conductive coolants provide a longer tool life by a factor of three due to the prevention of occurrence of tribo-plasma at the tool-workpiece interface. Goel et al. [22] employed distilled water in the ultraprecision machining of 6H-SiC but found significant wear marks and debris on the cutting edge. Chan et al. [23, 24] atomized the cutting fluid through nano-droplets (NDs) and found a better penetration into the cutting zone was achieved with lower surface waviness and roughness.

The effect of nanofluids on cutting process has been investigated by some researchers [25–27]. These nanofluids are obtained by mixing the nanoparticles into a base fluid [28]. Employing nanofluids can increase the viscosity and thermal conductivity of the coolant; and simultaneously, reduce the tool-workpiece friction [29, 30]. Nevertheless, the main limitation of these coolants are their higher cost, instability and agglomeration problems [31].

A few researchers also used gases for cooling [32, 33] and solid or semi-solid compounds such as wax sticks, bars, pastes, creams, and gels to cool and lubricate the machining area [34–36]. Such solid and semi-solid lubricants typically provide superior lubricity because of the higher adhesion to the cutting tool [37]. Also, in particular, the wax-based lubricants are cleaner and more environmentally friendly due to their benefits such as the reduction in lubricant usage, less spreading and easier collection, low odor, recyclability, and anti-corrosion characteristics [38, 39]. Solid lubricants with nanoparticles were also attempted in ultraprecision cutting of hard brittle materials. Yan et al. [40] dispersed four types of nanoparticles in lubrication grease and found that the grease with 10% Cu nanoparticles gave the best surface integrity as well as lowest tool wear in SiC cutting.

As the studies conducted on the effects of lubricants are still fewer compared to those on other factors of ultraprecision machining, there are great discrepancy in the reported

results. Therefore, the mechanisms of lubrication and cooling of various lubricants have not been clarified yet. In recent years, some researchers have examined the influence of cutting fluid using molecular dynamics (MD) method. An MD investigation considering the cutting atmosphere was conducted by Rentsch and Inasaki [41]. They focused on the heat convection by defining water atoms as the cutting fluid and found that a few fluid atoms could diffuse into the workpiece surface. Lautenschlaeger et al. [42] compared a lubricant with the vacuum atmosphere and found that a large part of the cutting tool was always in direct dry contact with the workpiece.

For silicon cutting, most researches have focused on liquid lubricants, while no study has examined the effect of solid and solid–liquid hybrid lubrication. In particular, there is no literature on lubricants for the microgrooving of silicon substrates yet. In a recent work by Heidari and Yan [43], a wax coating was used as an infiltrant in the ultraprecision machining of porous silicon, and the surface quality was found to be improved by reducing surface microfractures. This indicated the possibility of using wax coating as a lubricant for cutting hard brittle material, especially for microgrooving processes.

The aim of the present research is to investigate the influence of various cutting lubricants including liquid (oil), solid (wax coating) and solid–liquid (wax–oil) hybrid lubricants, on the cutting mechanism of arc-sectioned microgrooves of silicon. The changes in cutting forces, chip morphology, grooves topography and surface roughness, phase transformation, and chip adhesion were explored. The best cutting lubricants for achieving high-quality grooves at a low environmental load were identified.

2 Experimental Procedures

2.1 Workpiece

In this research, an N-type single crystalline silicon (100) wafer with the dimension of 50 mm × 50 mm × 0.7 mm was used as the specimen. As shown in Fig. 1, the specimen was attached on a copper jig using a wax at a tilting angle of about 0.1°. In each stage, the tool moved toward the wafer surface and entered into the workpiece up to 5 µm. Table 1 shows six lubrication conditions for microgroove cuttings. For this purpose, two types of waxes with different hardness and CASTY-LUBE®B-905 cutting oil were employed. The wax coatings were obtained by directly applying the melted wax on the workpiece with the thickness of about 2 mm, which was achieved by trial and error. The cutting oil was applied in two methods: oil mist jet and direct oil jet. In addition, the hybrid effect of the wax coating and oil

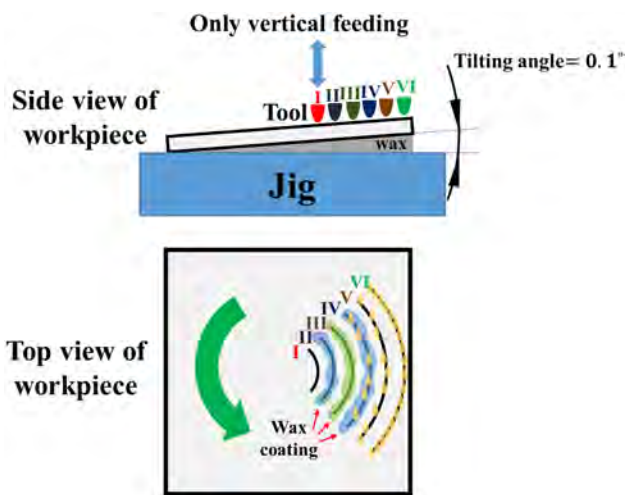


Fig. 1 Schematic view of silicon microgrooving under different lubrication conditions

was investigated. The characteristics of these materials are given in Table 2.

2.2 Cutting Tool

In the experiments, a round-nosed single-crystal diamond tool (Osaka Diamond CORP, Japan) with a nose radius of 1 mm and an edge radius of ~70 nm was employed. The rake and clearance angle of the tool was 0° and 15°, respectively. Arc-sectioned grooves were created in experiments. A fresh and intact cutting edge was utilized for microgrooving of each groove in order to exclude the effects of tool wear.

2.3 Machine Tool and Cutting Conditions

The microgrooving experiments were conducted on a three-axis (XZB) control ultraprecision machine, NACHI ASP-15 (NACHI-FUJIKOSHI CORP, Japan). The machine tool consists of two linear tables and one rotary table with hydrostatic bearings. Laser hologram scales are also employed for the accurate positioning of these tables. The linear and rotary resolutions of this machine equal 1 nm and 0.00001°, respectively. It is also equipped with an injection nozzle. For oil mist jet, the cutting oil is mixed with compressed air and sprayed onto the machining area through a nozzle. The main parts of the machine are illustrated in Fig. 2.

The parameters used in microgrooving experiments are listed in Table 3. Since different areas at various radial locations were used for each groove, the spindle rotation rate was

Table 2 Characteristics of the incorporated waxes and cutting oil

Wax 1	Wax 2	Cutting Oil			
Melting point (°C)	70	Melting point (°C)	95	Viscosity (40 °C, mm ² /s)	4.93
Hardness (HV)	3.11	Hardness (HV)	3.55	Density (15 °C, g/cm ³)	0.87

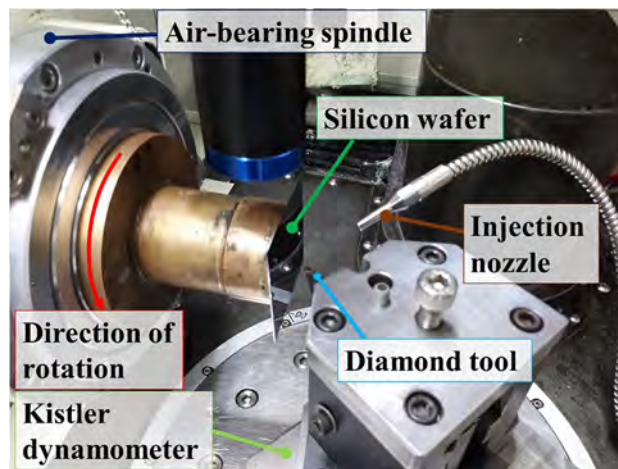


Fig. 2 Photograph of the microgrooving setup

Table 3 Arc grooving conditions

Machine tool	NACHI ASP-15
Total depth (<i>a</i>)	5 μm
Maximum undeformed chip thickness (<i>h</i> _{max})	500 nm
Feed rate (<i>f</i> _c)	13.5–45 μm/min
Cutting speed (<i>V</i> _c)	4 m/min
Spindle rotation rate (<i>N</i>)	27–90 rpm

adjusted in each step to maintain a constant cutting speed according to Eq. (1). On the other hand, a 500 nm fine depth of the cut was used for each workpiece rotation. Therefore, the tool was fed perpendicularly to the workpiece at a feed rate *f*_c (μm/min) as described by Eq. (2).

$$N = V_c / 2\pi r \tag{1}$$

$$f_c = V_c h_{max} / 2000\pi r \tag{2}$$

Table 1 Lubrication conditions applied in microgrooving

Groove number	I	II	III	IV	V	VI
Lubrication	Dry	Wax 1	Wax 2	Wax 1 + oil jet	Oil mist	Oil jet

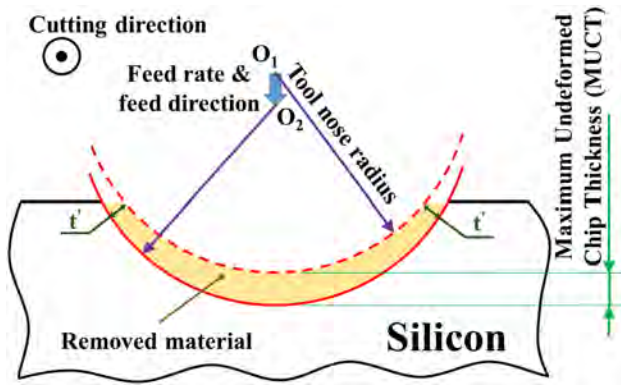


Fig. 3 Schematic diagram of the grooving model with an R-shaped tool

Figure 3 schematically shows the arc grooving model using an R-shaped diamond tool. In this figure the maximum undeformed chip thickness (MUCT) is equal to the tool advancement in one rotation. By focusing on the removed material, it can be observed that the chip thickness on the middle of the groove is a bit thicker than chip thickness on the groove edges ($MUCT > t'$).

2.4 Measurement Apparatus

The angle of the inclined workpiece on the copper jig was measured by an ultraprecision point autofocus probe (Mitaka, Japan). A micro Vickers hardness tester (Shimadzu HMV-G21S, Japan) was employed to measure the hardness of the wax coating. The cutting forces were picked up by a piezoelectric dynamometer (Kistler 9256C2) mounted under the tool holder. To evaluate the integrity of the grooves, a digital microscope (Keyence VH-Z100UR, Japan) and a white light interferometer Talysurf CCI1000 (AMETEK Taylor Hobson Ltd., UK) were used, and the surface profiles were analyzed by Talymap software. In addition, a laser micro-Raman spectrometer (JASCO NRS-3100, Japan) was employed to characterize the phase transformation. Finally, chip morphology and tool defects were examined by a field-emission scanning electron microscope (FE-SEM, Model Inspect F50).

3 Results and Discussion

3.1 Cutting Force Characteristics

The influence of the lubrication conditions on the force angle and average cutting force are plotted in Fig. 4. Force angle is defined as $\tan^{-1}(F_t/F_c)$, where F_t and F_c is the

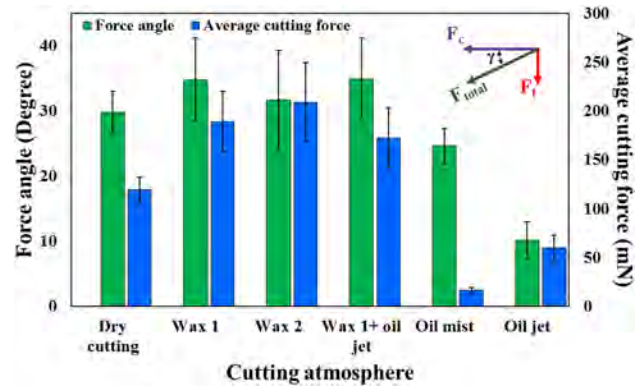


Fig. 4 Effect of lubrication conditions on the force angle and average cutting force

average thrust force and tangential force, respectively. As demonstrated in this figure, applying wax to the machined surface led to a comparable increase in the force angle, which is believed to be due to the lubricity effect (ability of a lubricant to reduce the average frictional coefficient) in the wax. Typically, this condition improves the surface characteristics [44, 45].

The amount of force angle drops by using the pure cutting oil, both in the oil mist and oil jet conditions. However, it is much more significant in the oil jet situation. At such low force angles, an appreciable deviation on the groove is expected.

While the wax coating and oil lubrication are simultaneously applied, the amount of force angle is closer to the sole wax coating condition. There may be two reasons for this issue. First, the amount of solid lubricant (wax layer) is much higher than the liquid lubricant (oil jet). Hence, the mechanics of cutting is mostly influenced by the wax layer. Second, the wax is embedded into the first layer of the workpiece and only a little amount of oil has the chance to penetrate into the grooving area due to the high cutting speed. The reason for the high force angle in the dry grooving mode will be explained later in Sect. 3.6.

As shown in Fig. 4, applying the wax coating on the workpiece surface results in an increase in the average cutting force. Although the silicon substrate is much harder than the wax lubricant, the thickness of the wax layer (~ 2 mm) is far larger than the maximum undeformed chip thickness of silicon (500 nm). For this reason, the presence of the wax layer leads to a considerable resistance to the grooving operation. In this circumstance, the harder wax (Wax2) causes a slightly higher cutting force. Due to the reduction of the tool-workpiece friction, the lowest cutting force is obtained in the oil mist condition. Under the oil jet condition, the cutting force is somewhat higher due to the chip adhesion phenomenon (Sect. 3.6).

3.2 Chip Morphology

Figure 5 presents the FE-SEM images of microchips obtained from dry microgrooving. Under this condition, long and continuous chips with arc-shaped cross-sections were created, indicating the predominance of the ductile phase machining. The reason for chips curvature was the different crystallographic directions during one workpiece rotation. The effect of crystallographic orientation on cutting forces has been widely studied by the previous researchers [46–48]. In the current experiments, although the cutting test is performed on a constant plane of Si (100), the cutting direction is changing continually with respect to the crystal structure; which leads to successive changes in the stress state. Subsequently, the direction of chip flow is changing during the machining process, and as a result, the curved chips are achieved. Because of the lower chip width in the initial passes, this issue was more significant; and the rose-shaped chip was created (Fig. 5b). Changes in the cutting direction, along with the side flow and vibration of the cutting forces, result in the chip edge tearing. A portion of these separated parts was capable of sticking to the freshly-machined surface as the debris and declining the final surface finish.

The FE-SEM image of cutting chip in the “wax 1” coating mode is displayed in Fig. 6. Interestingly, a discontinuous chip was created. This issue led to more fluctuations in the cutting forces and consequently, a wider error bar can be found in force angle in Fig. 4.

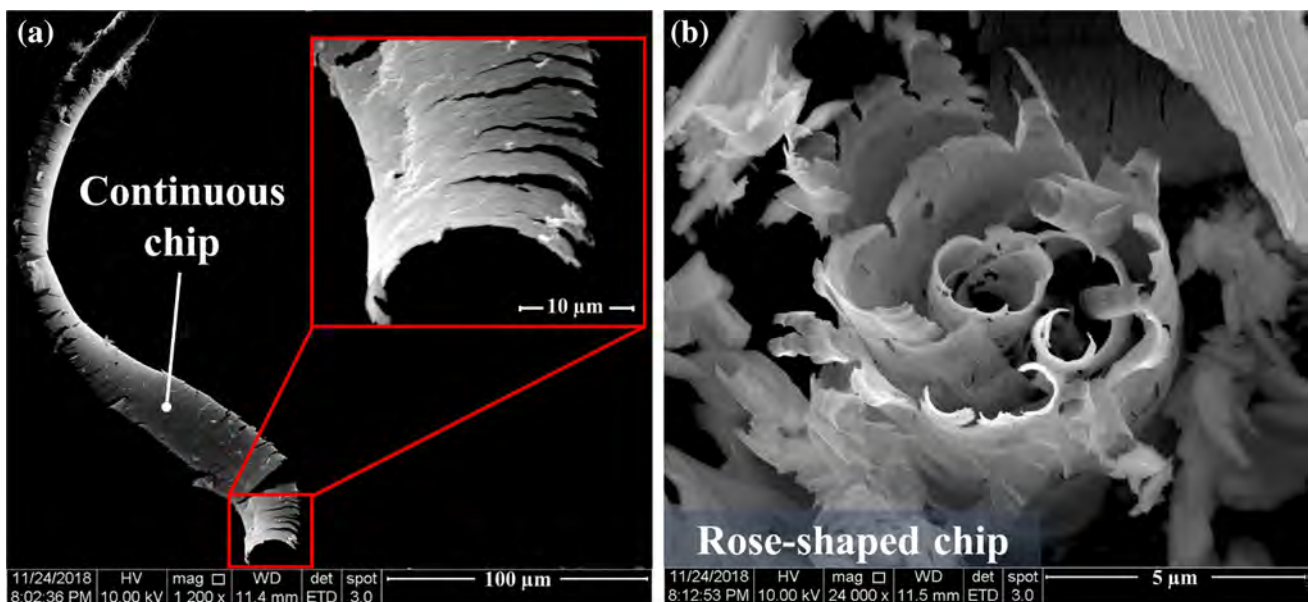


Fig. 5 FE-SEM micrographs of the chips in the dry condition

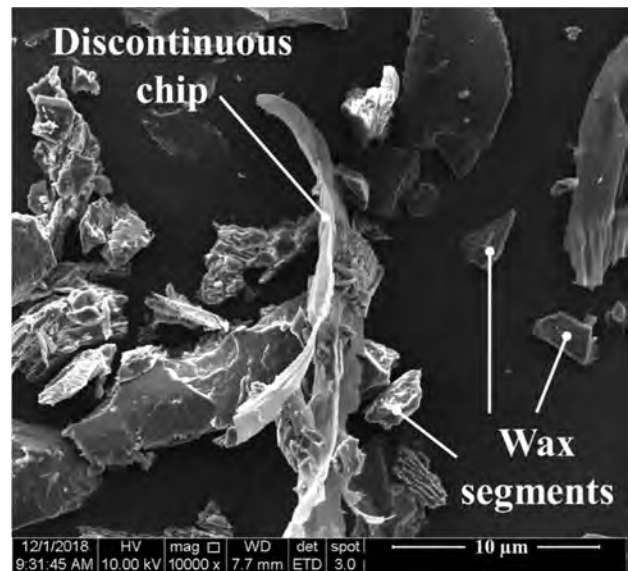


Fig. 6 FE-SEM micrographs of the chips in the wax (type 1) coating condition

Nevertheless, the creation of discontinuous chips is considered to be due to the contact pressure from the wax coating and does not mean the existence of the brittle mode machining. Although the achievement of continuous chips is a positive indication of the ductile mode cutting, their existence is not always desirable. Such continuous and long chips can become entangled with the cutting tool tip and reduce tool life and surface integrity [49].

3.3 Groove Topography

Figure 7 demonstrates the effect of different lubrication conditions on the entrance and exit of the cutting tool. In general, grooves have better quality at the entrance. In this circumstance, the effective rake angle is higher than the nominal one due to the effect of edge radius; as a result, the contact pressure between the tool and machined silicon surface grows. In such a case, the high-pressure phase transformation (HPPT) is induced more easily, and the ductile mode cutting is achieved. In contrast, the effective rake angle in the exit area is less than the nominal value. Moreover, unlike the entrance side (which is under compression), the stress situation in the exit side is tensile. These issues could cause fluctuations in the cutting force, leading to earlier brittle mode cutting. Additionally, a part of grooved chips enters the cutting area and deteriorates the exit surface quality.

Comparing the wax coating conditions with others, it demonstrates that a highly ductile regime grooving occurs, both in the entrance and exit areas. There are two main reasons for this: The first reason is the breaking of the chips which reduces the risk of the damage caused by continuous chips. The second is the role of the wax coating as a lubricant which reduces the frictional forces.

Figure 8 shows the chip formation mechanism of silicon workpiece in the presence of a layer of wax. As the cutting process proceeds, the chip is created in front of the tool (Fig. 8b). In this situation, the pressure induced by the chip formation causes a pile-up and a few cracks in the wax layer above the tool. On the other hand, the wax provides resistance to the normal flow of the chip. This issue, along with the difference in the chip-tool and chip-wax friction coefficients, will result in creation of stress and micro-cracks in the chip area. Subsequently, by more tool advancement, the chip is broken and the surrounded wax is disintegrated (Fig. 8c). However, due to the presence of the wax layer, the breakage impact and the ejection of the cutting chip are controlled, to some extent. In this circumstance, a part of disintegrated wax particles enters into the tool edge and rake face areas, which acts as the solid lubricant (Fig. 8d). Therefore, better surface quality would be achieved.

It is worth noting that, when the oil was used, the surface quality of the grooves entrance and exit decreased. The reason for the fluctuations in the cross-sectional exit profiles in these conditions can be explained by trapping the chips particles due to the viscosity of the cutting oil in front of the tool. The results also exhibited that, while the wax coating and oil jet were applied simultaneously, the groove topography in the entrance and exit areas was mostly affected by the wax layer, rather than the cutting oil.

Figure 9 demonstrates a comparison of groove topographies in Wax1 and Wax1 + oil jet conditions. In the case of the sole wax coating, despite the presence of some

fractures, the main cutting regime is in the ductile mode. Moreover, there is no burr formation on the edges of all grooves because chip thickness is almost constant along the groove width. In this way, the cutting conditions at both sides of the groove edges are similar to the orthogonal cutting situation with the fluent material flow. However, under the hybrid lubrication, the quality of groove center is drastically affected and degraded by the oil jet. The reason of this issue will be explained in Sect. 3.4.

The surface topography obtained from dry grooving and the related cross-sectional profiles along different directions are depicted in Fig. 10. The effect of micro-fractures can be observed, and the dominant cutting mechanism in the middle of the groove seems to be under the brittle mode.

The roughness of groove fringes at the two sides of the groove slightly differs. There are two reasons for this: Firstly, the cutting speed on the two edges is a little different due to the different cutting diameters, and secondly, there is slight unevenness along the cutting-edge radius.

3.4 Groove Surface Roughness

A comparison of groove bottom and fringe roughness under different lubrication conditions is given in Fig. 11. In all conditions, the fringe roughness is higher than the bottom roughness. This is presumably caused by the side flow of material at the edges. Furthermore, owing to the analyses presented in Sect. 3.3, inequality of the groove fringes is also observed in other lubrication conditions. However, the wax coating conditions present a different trend: higher surface roughness in the outer fringe than the inner fringe. There are two possible reasons for this issue. Firstly, due to the higher cutting speed in the outer fringe, the disintegration impact of wax particles is slightly higher. Secondly, owing to the centrifugal force, the disintegrated wax particles in the groove bottom tend to be thrown toward the outer fringe. Therefore, the outer fringe is subjected to higher disturbances, which results in a higher surface roughness.

Known from Fig. 4, using the cutting oil results in a reduction in machining forces and, as a consequent, an improvement in the final groove integrity. However, the roughness of groove bottom in the oil jet condition is slightly less than that in the oil mist situation. Under this condition, the grooving chips are more likely to remain in the cut area and, subsequently, the possibility of their abrasive effects on the grooved surface increases. Another drawback of this lubrication method is the increased consumption of cutting oil by machining, and consequently, augmentation of environmental pollution and health problems.

The best groove finish was achieved by wax coating. In this circumstance, the roughness of groove bottom is around 11.6 nm which is almost 11 and 8 times smoother than the dry and wet (oil mist/oil jet) cutting, respectively. The first

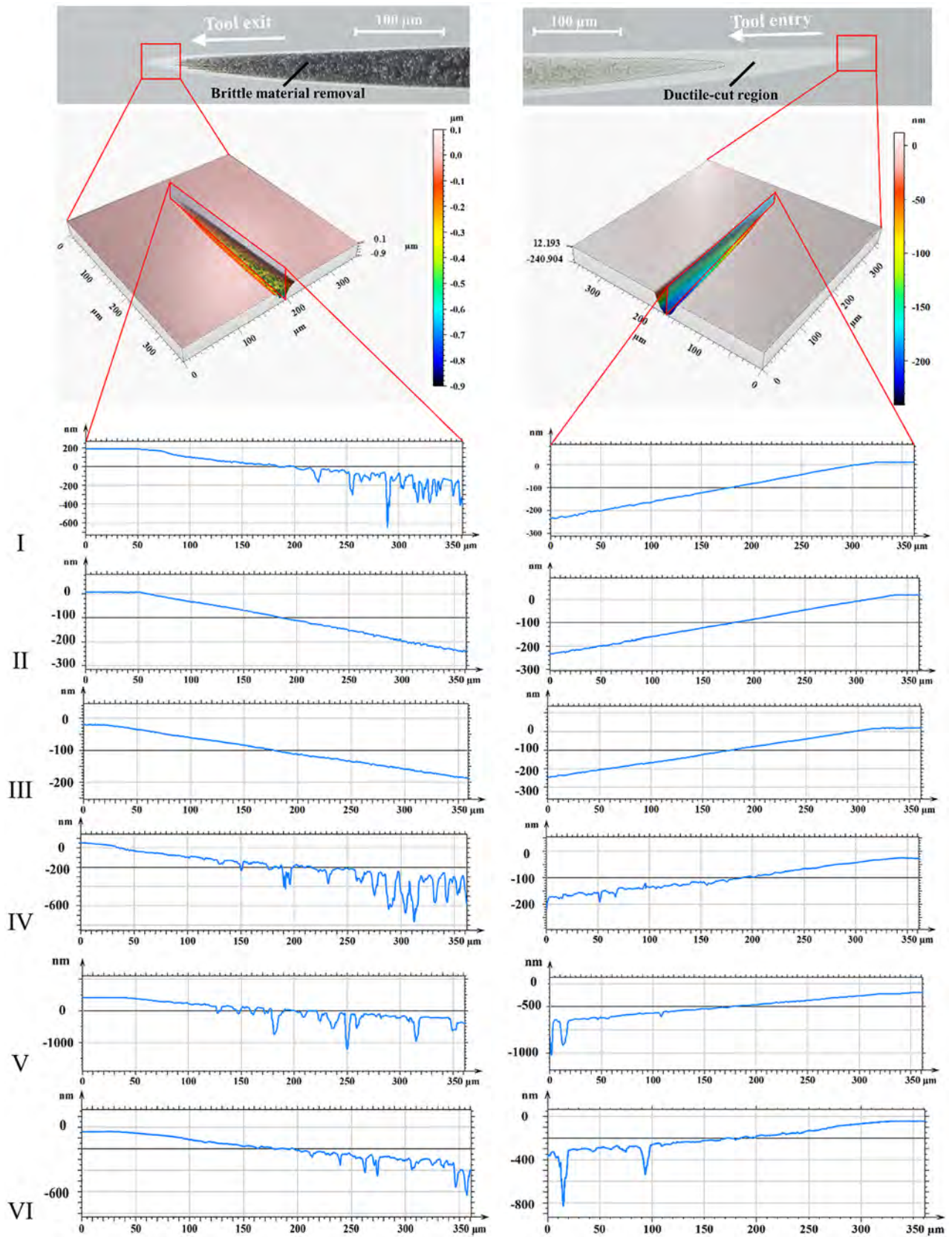


Fig. 7 The effect of lubrication conditions on the entrance and exit of the tool

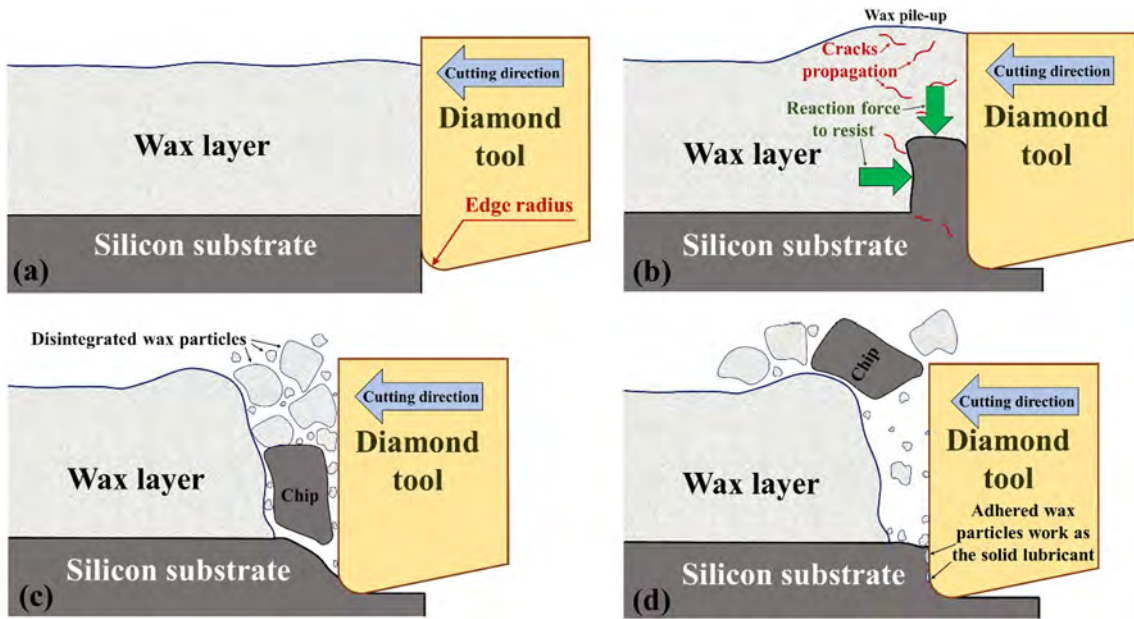


Fig. 8 Effect of wax coating on chip formation: **a** entrance of the tool, **b** cracks propagation in wax and chip, **c** disintegration of the wax and chip breakage, **d** adhesion of the wax particles on the tool edge and rake face and working as the solid lubricant

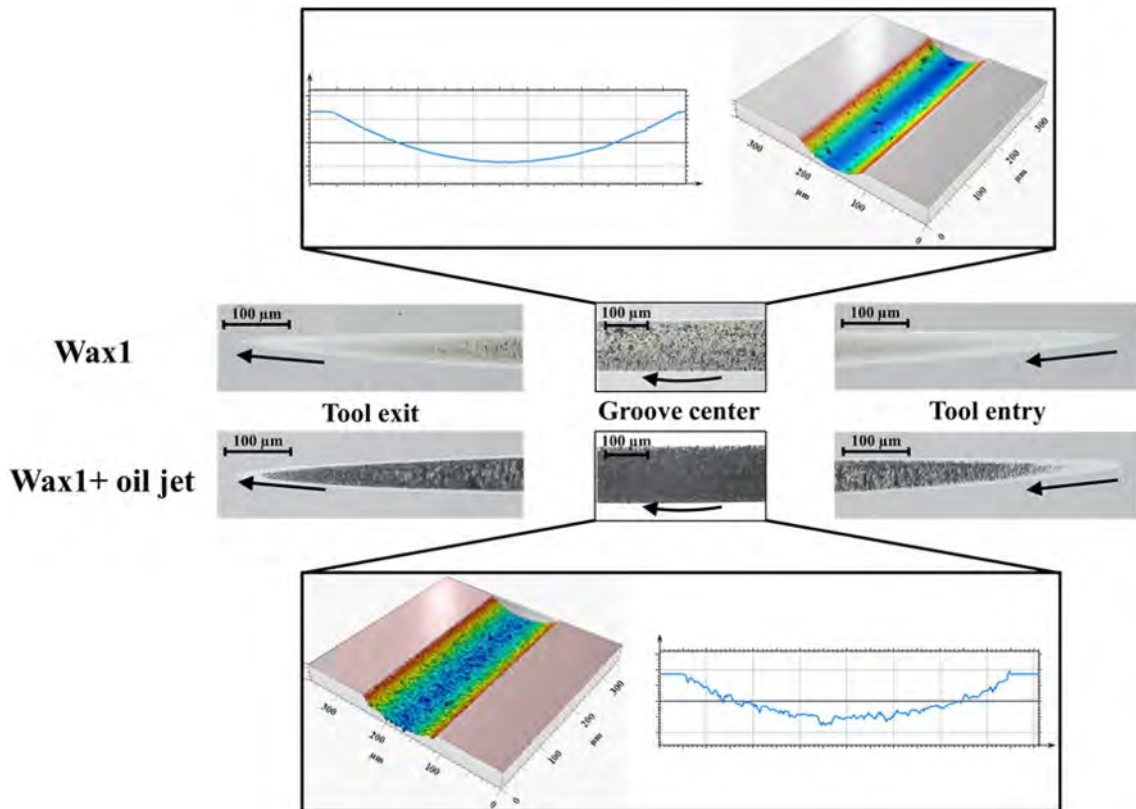


Fig. 9 Surface topography and cross-sectional view of groove in Wax1 coating, and Wax1 + oil jet conditions

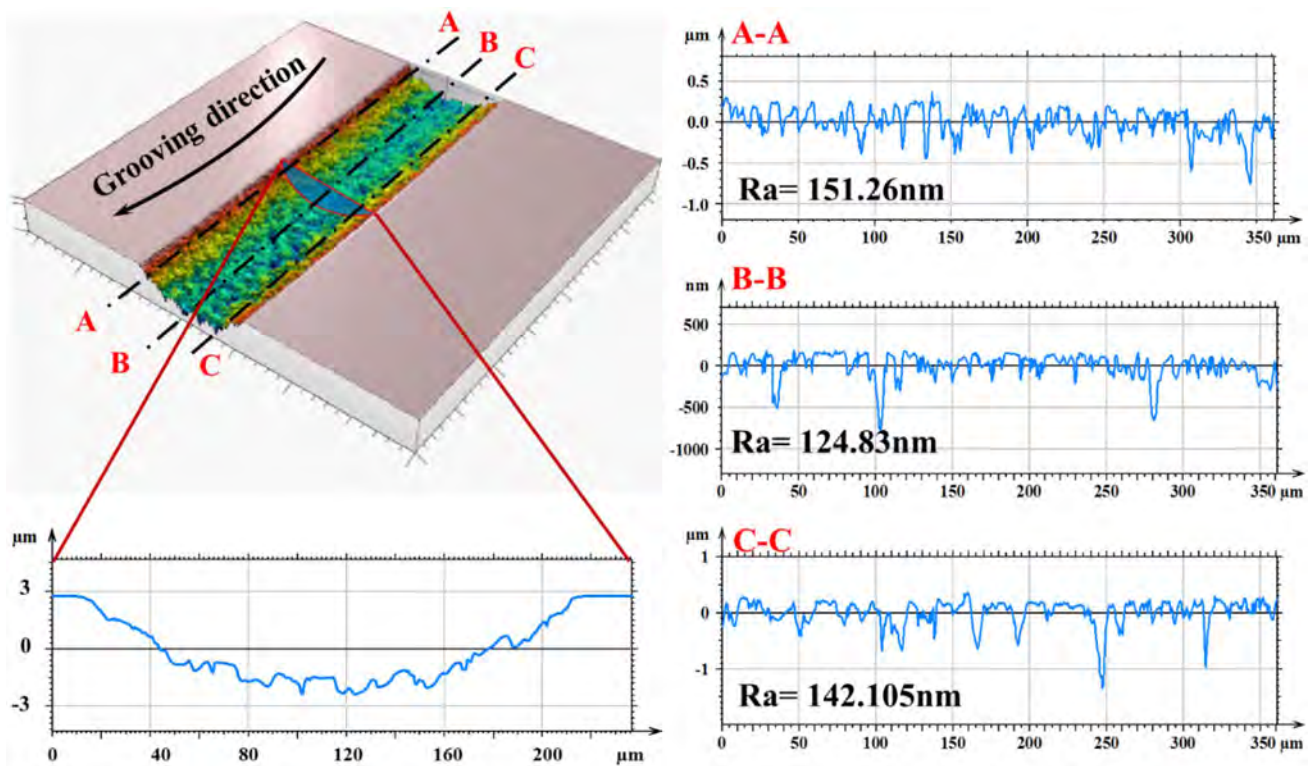


Fig. 10 Surface topography of dry grooving and the related cross-sections

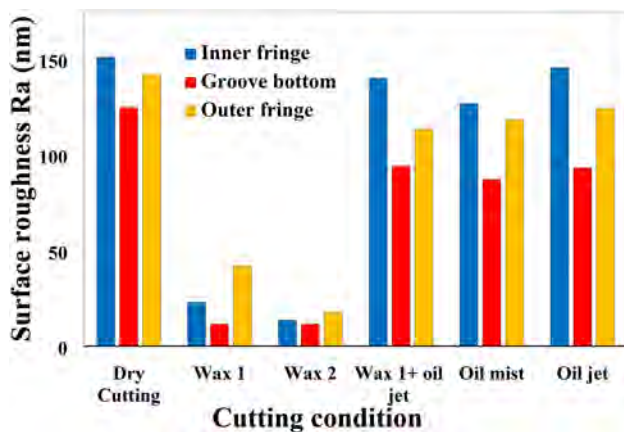


Fig. 11 Effect of lubrication conditions on the groove roughness

reason for this is the role of chip breaker played by the wax coating. In such cases, the discontinuous chips are created during the ductile regime grooving, providing an ideal situation for the machining of hard and brittle materials. Besides that, the stability of the cutting environment is a key factor in achieving a higher form accuracy and better surface roughness [50]. Clinging of the lubricant particles to the tool and workpiece is a significant parameter which can affect this. In the application of the wax coating, the workpiece surface is

uniformly covered with a solid lubricant (wax). This implies that the wax particles have more chance to enter the tool-workpiece interface and improve the groove quality.

Under the hybrid condition (wax1 + oil jet), the surface roughness is closer to the sole oil condition than the wax coating. It is probably because the disintegrated wax and chip particles remain in the cutting area due to the oil viscosity. In this way, a part of these particles enters into the tool-workpiece interface and reduce the final quality.

A noteworthy finding is that using the wax with higher hardness and melting point leads to a better result. It can be stated that this has occurred because of higher environmental stability in such a situation.

3.5 Material Phase Transformation

Figure 12 presents the Raman spectral mapping of normalized amorphization intensity for the start, middle, and end of the grooves under the dry condition and “wax 1” coating. The normalized peak height was calculated at 470 cm^{-1} from the Raman shift ranging from 100 to 800 cm^{-1} . The red color (up-shift of Raman band) represents a higher amorphization intensity [51].

Previous studies have proved that during the brittle mode machining, the cutting mechanism is based on the expansion of the brittle fractures and, in such a case, there

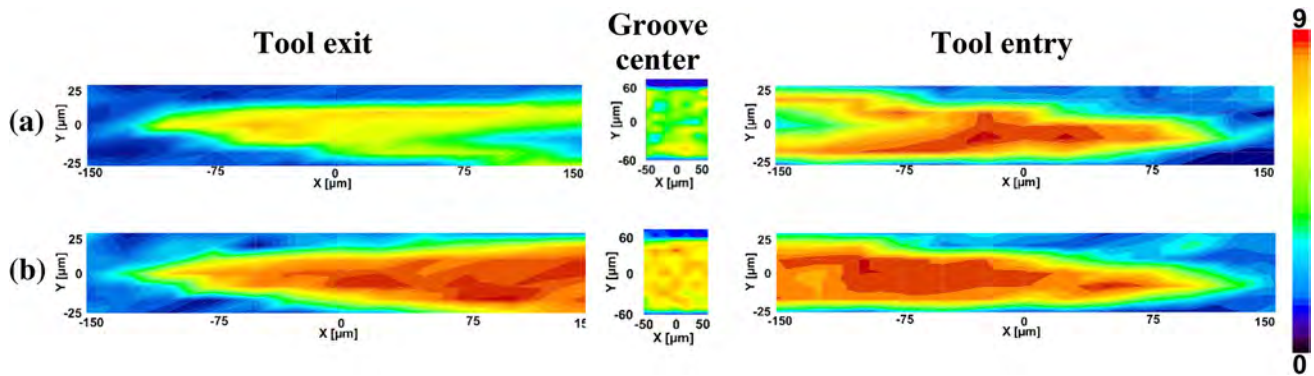


Fig. 12 Submicron Raman intensity maps of the peak height of amorphous silicon under **a** dry grooving, and **b** wax coating

is no phase transformation [52]. On the contrary, phase transformation can be found under the ductile mode cutting in brittle materials. This means that ductile mode machining is not necessarily a damage-free process due to the high pressure-induced metallization under the tool. As demonstrated in Fig. 12, the tool entry is always under higher phase transformation than the exit region, indicating the dominance of the ductile mode cutting in the entrance area. This result is consistent with the groove roughness presented in Fig. 7. Furthermore, based on Fig. 12b, the peak heights of the amorphous silicon increased under the wax coating condition; thus, further processing-induced phase transformation was produced. Therefore, it can be claimed once more that the use of wax coating further expands the ductile machinability. The groove roughness values presented in Fig. 11 also confirms this result.

3.6 Chip Adhesion

The quality of the cutting edge can directly affect the ductile machinability of a brittle material, such as silicon. Examining the FE-SEM images along the cutting edge demonstrated that there is no chip adhesion in the wax coating and oil mist conditions. As discussed earlier in Sect. 3.3, under the wax coating condition, the cutting edge is in continuous and sufficient nourishment of disintegrated wax. In the oil mist condition, the fine droplets of cutting oil can easily enter into the cutting zone. Nevertheless, there is a slight chip adhesion on the cutting edge under dry grooving (Fig. 13a) as well as hybrid lubrication (Fig. 13b). This could be another reason in creation of the curved chip, which was already discussed in Sect. 3.2. Figure 14 illustrates the scheme of the two-dimensional material flow in arc grooving. Evidently, owing to the high hydrostatic pressure caused by the stagnation region on the tool apex, this area is highly susceptible to

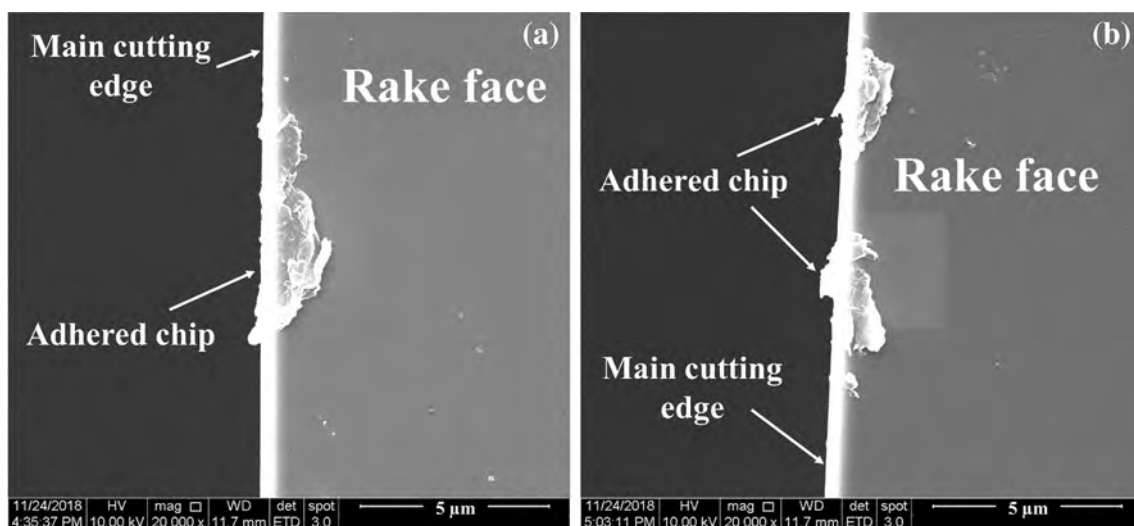


Fig. 13 High-magnification FE-SEM photography of the chip adhered on the cutting edge: **a** dry grooving, **b** hybrid lubrication (wax coating and oil jet)

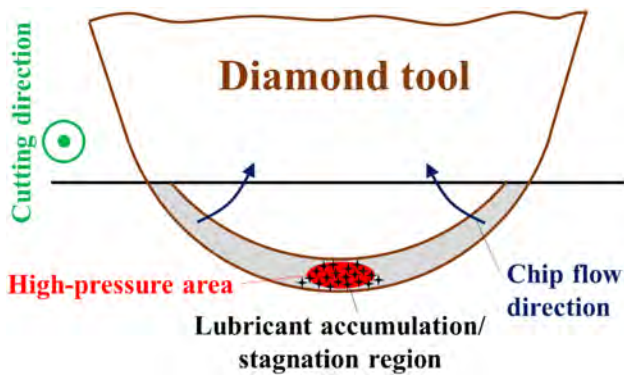


Fig. 14 The 2-D model of material flow and lubricant accumulation (under wet machining)

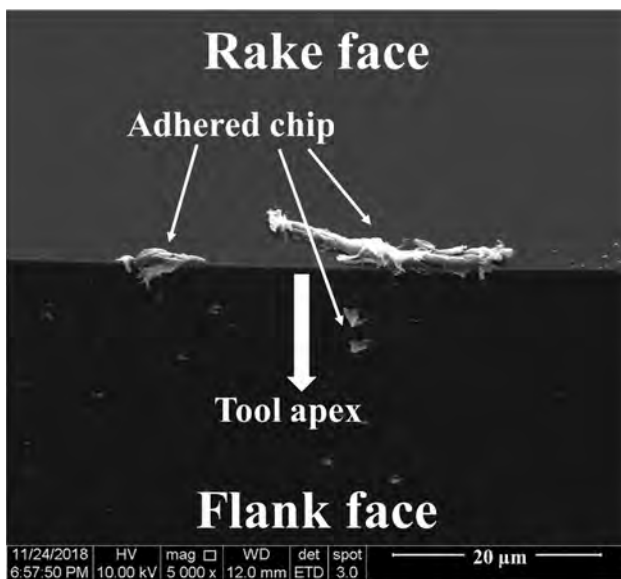


Fig. 15 FE-SEM photography of chip adhesion on the cutting edge under oil jet condition

material adhesion. Under the dry grooving, the size of the adhered chip is larger than the grooving depth. Subsequently, this adhered layer increases the friction during chip flow, which leads to an increase in the thrust force, thereby boosting the force angle (Fig. 4).

The morphology of the adhered chips in these two conditions is largely similar to each other. Nonetheless, in terms of using hybrid lubrication (wax coating and oil jet), chip adhesion does not occur at the tool apex. Under this condition, lubricant accumulation occurs due to the stagnation phenomenon (Fig. 14). Thus, this part of the tool always has an adequate supply of lubrication. On the two sides of the tool apex, on the other hand, the presence of cutting oil on the wax coating results in an easier sliding in the wax

particles. As a result, the lubricity of the wax drops and a slight chip adhesion is generated in these areas.

As indicated in Fig. 15, the same result was observed under the oil jet condition. Therefore, the roughness values of grooves fringe and bottom are very close in IV and VI conditions. In this situation, the pressure induced by the wax coating is not present, and the separated particles resulting from chip edge tearing are retained by the adhesion of the oil in the grooving locus. This issue along with the disparity in lubrication performance leads to a different configuration in the adhered chips.

The use of wax coating as lubricant has several advantages. First, it is easier to apply the wax coating uniformly on the workpiece surface than providing oil or oil mist to the cutting point precisely. Second, the consumption amount of wax is very little by selectively applying the melted wax only on the machining area. Third, there is almost no pollution to air and no contamination to machine tools. Fourth, it is easy to separate wax and silicon by heating their mixture and recycling both of them. Therefore, wax coating might provide an environmentally friendly method for lubrication of hard brittle materials cutting, and contribute to the realization of green manufacturing.

4 Conclusions

The effects of various cutting lubricants were examined on microgrooving of single-crystal silicon. The following conclusions were drawn:

- Wax coating acts as a chip breaker and breaks the continuous chips, which enhances the ductile machinability and intensifies the grooving-induced phase transformation.
- For all lubricating methods, the entrance side of the microgroove is always smoother than the exit side with more phase transformation. The groove bottom is always smoother than the fringes.
- Using a harder wax coating decreases the roughness in the groove fringes and increases the uniformity of the surface roughness of a groove.
- The use of cutting oil, regardless in the form of oil jet or mist jet, improves the groove roughness.
- Chip adhesion is significant under dry cutting as well as oil lubrication.
- The best lubrication performance is achieved by wax coating, where chip adhesion does not occur and surface roughness improves by a factor of ~ 11 .
- Raman spectral mapping show that the use of wax coating further expands the ductile machinability in microgrooving silicon.

Future research could investigate the effect of wax lubrication on ultraprecision interrupted cutting of silicon wafer to achieve a fully machined surface.

References

- Chen, Y.-L., Cai, Y., Shimizu, Y., Ito, S., Gao, W., & Ju, B.-F. (2016). Ductile cutting of silicon microstructures with surface inclination measurement and compensation by using a force sensor integrated single point diamond tool. *Journal of Micro-mechanics and Microengineering*, 26(2), 025002. <https://doi.org/10.1088/0960-1317/26/2/025002>.
- Sun, Z., To, S., & Zhang, S. (2018). A novel ductile machining model of single-crystal silicon for freeform surfaces with large azimuthal height variation by ultra-precision fly cutting. *International Journal of Machine Tools and Manufacture*, 135(July), 1–11. <https://doi.org/10.1016/j.ijmactools.2018.07.005>.
- Ameli Kalkhoran, S. N., Vahdati, M., & Yan, J. (2019). Molecular dynamics investigation of nanometric cutting of single-crystal silicon using a blunt tool. *JOM Journal of the Minerals Metals and Materials Society*, 71(12), 4296–4304. <https://doi.org/10.1007/s11837-019-03671-w>.
- Davim, J. P. (2010). *Surface integrity in machining*. London: Springer. <https://doi.org/10.1007/978-1-84882-874-2>.
- Kaynak, Y., Lu, T., & Jawahir, I. S. (2014). Cryogenic machining-induced surface integrity: A review and comparison with dry, mql, and flood-cooled machining. *Machining Science and Technology*. <https://doi.org/10.1080/10910344.2014.897836>.
- Wang, M., Wang, W., & Lu, Z. (2012). Critical cutting thickness in ultra-precision machining of single crystal silicon. *International Journal of Advanced Manufacturing Technology*. <https://doi.org/10.1007/s00170-012-4222-0>.
- Abdulkadir, L. N., Abou-El-Hossein, K., Jumare, A. I., Odedeyi, P. B., Liman, M. M., & Olaniyan, T. A. (2018). Ultra-precision diamond turning of optical silicon—A review. *The International Journal of Advanced Manufacturing Technology*. <https://doi.org/10.1007/s00170-017-1529-x>.
- Karpat, Y. (2019). Influence of diamond tool chamfer angle on surface integrity in ultra-precision turning of single crystal silicon. *The International Journal of Advanced Manufacturing Technology*, 101(5–8), 1565–1572. <https://doi.org/10.1007/s00170-018-3053-z>.
- El Baradie, M. A. (1996). Cutting fluids: Part I. Characterisation. *Journal of Materials Processing Technology*, 56(1–4), 786–797. [https://doi.org/10.1016/0924-0136\(95\)01892-1](https://doi.org/10.1016/0924-0136(95)01892-1).
- Heidari, M., & Yan, J. (2018). Material removal mechanism and surface integrity in ultraprecision cutting of porous titanium. *Precision Engineering*, 52, 356–369. <https://doi.org/10.1016/j.precisioneng.2018.01.014>.
- Liew, P. J., Shaaroni, A., Sidik, N. A. C., & Yan, J. (2017). An overview of current status of cutting fluids and cooling techniques of turning hard steel. *International Journal of Heat and Mass Transfer*, 114, 380–394. <https://doi.org/10.1016/j.ijheatmasstransfer.2017.06.077>.
- Yan, J., Sasaki, T., Tamaki, J., Kubo, A., & Sugino, T. (2004). Chip formation behaviour in ultra-precision cutting of electroless nickel plated mold substrates. *Key Engineering Materials*, 257–258, 3–8. <https://doi.org/10.4028/www.scientific.net/KEM.257-258.3>.
- Zou, L., Huang, Y., Zhou, M., & Yang, Y. (2017). Effect of cryogenic minimum quantity lubrication on machinability of diamond tool in ultraprecision turning of 3Cr2NiMo steel. *Materials and Manufacturing Processes*, 6914(September), 1–7. <https://doi.org/10.1080/10426914.2017.1376077>.
- Garside, M. (2019). *Lubricants—Statistics & facts*. Retrieved December 18, 2019, from <https://www.statista.com/topics/5263/lubricants-industry/>.
- Theodori, D., Saft, R. J., Krop, H., & van Broekhuizen, P. (2004). *Development of criteria for the award of the European Eco-label to lubricants*. Retrieved December 18, 2019, from <http://www.ivam.uva.nl/>.
- Danyluk, S., & Reaves, R. (1982). Influence of fluids on the abrasion of silicon by diamond. *Wear*, 77(1), 81–87. [https://doi.org/10.1016/0043-1648\(82\)90047-3](https://doi.org/10.1016/0043-1648(82)90047-3).
- Moriwaki, T., Horiuchi, A., & Okuda, K. (1990). Effect of cutting heat on machining accuracy in ultra-precision diamond turning. *CIRP Annals*, 39(1), 81–84. [https://doi.org/10.1016/S0007-8506\(07\)61007-5](https://doi.org/10.1016/S0007-8506(07)61007-5).
- Yan, J., Syoji, K., & Tamaki, J. (2003). Some observations on the wear of diamond tools in ultra-precision cutting of single-crystal silicon. *Wear*, 255(7–12), 1380–1387. [https://doi.org/10.1016/S0043-1648\(03\)00076-0](https://doi.org/10.1016/S0043-1648(03)00076-0).
- Yan, J., Tamaki, J., Syoji, K., & Kuriyagawa, T. (2004). Single-point diamond turning of CaF₂ for nanometric surface. *The International Journal of Advanced Manufacturing Technology*, 24(9–10), 640–646. <https://doi.org/10.1007/s00170-003-1747-2>.
- Davim, J. P., & Jackson, M. J. (2009). *Nano and micromachining* (Vol. 91). London: Wiley.
- Ohta, T., Yan, J. W., Kodera, S., Yajima, S., Horikawa, N., Takahashi, Y., et al. (2008). Coolant effects on tool wear in machining single-crystal silicon with diamond tools. *Key Engineering Materials*, 389–390, 144–150. <https://doi.org/10.4028/www.scientific.net/KEM.389-390.144>.
- Goel, S., Luo, X., Comley, P., Reuben, R. L., & Cox, A. (2013). Brittle-ductile transition during diamond turning of single crystal silicon carbide. *International Journal of Machine Tools and Manufacture*, 65, 15–21. <https://doi.org/10.1016/j.ijmactools.2012.09.001>.
- Chan, C. Y., Lee, W. B., & Wang, H. (2013). Enhancement of surface finish using water-miscible nano-cutting fluid in ultra-precision turning. *International Journal of Machine Tools and Manufacture*, 73, 62–70. <https://doi.org/10.1016/j.ijmactools.2013.06.006>.
- Chan, C. Y., Li, L. H., Lee, W. B., & Wong, H. C. (2016). Use of nano-droplet-enriched cutting fluid (NDCF) in ultra-precision machining. *The International Journal of Advanced Manufacturing Technology*, 84(9–12), 2047–2054. <https://doi.org/10.1007/s00170-015-7861-0>.
- Hegab, H., Umer, U., Soliman, M., & Kishawy, H. A. (2018). Effects of nano-cutting fluids on tool performance and chip morphology during machining Inconel 718. *The International Journal of Advanced Manufacturing Technology*, 96(9–12), 3449–3458. <https://doi.org/10.1007/s00170-018-1825-0>.
- Wang, Y., Li, C., Zhang, Y., Yang, M., Li, B., Dong, L., et al. (2018). Processing characteristics of vegetable oil-based nano-fluid MQL for grinding different workpiece materials. *International Journal of Precision Engineering and Manufacturing-Green Technology*, 5(2), 327–339. <https://doi.org/10.1007/s40684-018-0035-4>.
- Musavi, S. H., Davoodi, B., & Niknam, S. A. (2019). Effects of reinforced nanofluid with nanoparticles on cutting tool wear morphology. *Journal of Central South University*, 26(5), 1050–1064. <https://doi.org/10.1007/s11771-019-4070-2>.
- Saidur, R., Leong, K. Y., & Mohammed, H. A. (2011). A review on applications and challenges of nanofluids. *Renewable and Sustainable Energy Reviews*, 15(3), 1646–1668. <https://doi.org/10.1016/j.rser.2010.11.035>.

29. Srikant, R. R., Rao, D. N., Subrahmanyam, M. S., & Krishna, V. P. (2009). Applicability of cutting fluids with nanoparticle inclusion as coolants in machining. *Proceedings of the Institution of Mechanical Engineers, Part J: Journal of Engineering Tribology*, 223(2), 221–225. <https://doi.org/10.1243/13506501JET463>.
30. Sharma, A. K., Tiwari, A. K., & Dixit, A. R. (2015). Progress of nanofluid application in machining: A review. *Materials and Manufacturing Processes*, 30(7), 813–828. <https://doi.org/10.1080/10426914.2014.973583>.
31. Mahian, O., Kianifar, A., Kalogirou, S. A., Pop, I., & Wongwises, S. (2013). A review of the applications of nanofluids in solar energy. *International Journal of Heat and Mass Transfer*, 57(2), 582–594. <https://doi.org/10.1016/j.ijheatmasstransfer.2012.10.037>.
32. Shokrani, A., Dhokia, V., & Newman, S. T. (2012). Environmentally conscious machining of difficult-to-machine materials with regard to cutting fluids. *International Journal of Machine Tools and Manufacture*, 57, 83–101. <https://doi.org/10.1016/j.ijmachtools.2012.02.002>.
33. Chavoshi, S. Z., Gallo, S. C., Dong, H., & Luo, X. (2017). High temperature nanoscratching of single crystal silicon under reduced oxygen condition. *Materials Science and Engineering A*, 684(August 2016), 385–393. <https://doi.org/10.1016/j.msea.2016.11.097>.
34. Hoffman, P. J., Hopewell, E. S., Janes, B., Kent, M., & Sharp, J. (2011). *Precision machining technology*. Delmar: Montreal.
35. Jianxin, D., Ze, W., Yunsong, L., Ting, Q., & Jie, C. (2012). Performance of carbide tools with textured rake-face filled with solid lubricants in dry cutting processes. *International Journal of Refractory Metals & Hard Materials*, 30(1), 164–172. <https://doi.org/10.1016/j.ijrmhm.2011.08.002>.
36. Kotkowiak, M., Piasecki, A., & Kulka, M. (2019). The influence of solid lubricant on tribological properties of sintered Ni–20%CaF₂ composite material. *Ceramics International*. <https://doi.org/10.1016/j.ceramint.2019.05.262>.
37. Dilbag, S., & Rao, P. V. (2008). Performance improvement of hard turning with solid lubricants. *The International Journal of Advanced Manufacturing Technology*, 38(5–6), 529–535. <https://doi.org/10.1007/s00170-007-1079-8>.
38. Li, W., Kong, X. H., Ruan, M., Ma, F. M., Zuo, X. H., & Chen, Y. (2012). Green tribological behavior of waxes, adhesives and lubricants. In M. Nosonovsky & B. Bhushan (Eds.), *Green tribology. Green energy and technology* (pp. 393–411). Berlin: Springer. https://doi.org/10.1007/978-3-642-23681-5_14.
39. Hsu, C. S., & Robinson, P. R. (2019). Lubricant processes and synthetic lubricants. In *Petroleum science and technology* (pp. 253–285). Cham: Springer International Publishing. https://doi.org/10.1007/978-3-030-16275-7_13.
40. Yan, J., Zhang, Z., & Kuriyagawa, T. (2011). Effect of nanoparticle lubrication in diamond turning of reaction-bonded SiC. *International Journal of Automation Technology*, 5(3), 307–312. <https://doi.org/10.20965/ijat.2011.p0307>.
41. Rentsch, R., & Inasaki, I. (2006). Effects of fluids on the surface generation in material removal processes. *CIRP Annals*, 55(1), 601–604. [https://doi.org/10.1016/S0007-8506\(07\)60492-2](https://doi.org/10.1016/S0007-8506(07)60492-2).
42. Lautenschlaeger, M. P., Stephan, S., Urbassek, H. M., Kirsch, B., Aurich, J. C., Horsch, M. T., et al. (2017). Effects of lubrication on the friction in nanometric machining processes: A molecular dynamics approach. *Applied Mechanics and Materials*, 869, 85–93. <https://doi.org/10.4028/www.scientific.net/AMM.869.85>.
43. Heidari, M., & Yan, J. (2017). Ultraprecision surface flattening of porous silicon by diamond turning. *Precision Engineering*, 49, 262–277. <https://doi.org/10.1016/j.precisioneng.2017.02.015>.
44. Mukaida, M., & Yan, J. (2017). Ductile machining of single-crystal silicon for microlens arrays by ultraprecision diamond turning using a slow tool servo. *International Journal of Machine Tools and Manufacture*, 115(July 2016), 2–14. <https://doi.org/10.1016/j.ijmachtools.2016.11.004>.
45. Heidari, M., & Yan, J. (2018). Nanometer-scale chip formation and surface integrity of pure titanium in diamond turning. *The International Journal of Advanced Manufacturing Technology*, 95(1–4), 479–492. <https://doi.org/10.1007/s00170-017-1185-1>.
46. Yan, J., Asami, T., Harada, H., & Kuriyagawa, T. (2012). Crystallographic effect on subsurface damage formation in silicon microcutting. *CIRP Annals - Manufacturing Technology*, 61(1), 131–134. <https://doi.org/10.1016/j.cirp.2012.03.070>.
47. Wang, Z., Chen, J., Wang, G., Bai, Q., & Liang, Y. (2017). Anisotropy of single-crystal silicon in nanometric cutting. *Nanoscale Research Letters*, 12(1), 300. <https://doi.org/10.1186/s11671-017-2046-4>.
48. Liu, B., Xu, Z., Chen, C., Li, R., Wang, C., & Yang, X. (2019). In situ experimental study on material removal behaviour of single-crystal silicon in nanocutting. *International Journal of Mechanical Sciences*, 152(January), 378–383. <https://doi.org/10.1016/j.ijmecsci.2019.01.015>.
49. Ezugwu, E. O. (2005). Key improvements in the machining of difficult-to-cut aerospace superalloys. *International Journal of Machine Tools and Manufacture*, 45(12–13), 1353–1367. <https://doi.org/10.1016/j.ijmachtools.2005.02.003>.
50. To, S. S., Wang, H., & Lee, W. B. (2018). *Materials characterisation and mechanism of micro-cutting in ultra-precision diamond turning. Materials characterisation and mechanism of micro-cutting in ultra-precision diamond turning*. Berlin: Springer. <https://doi.org/10.1007/978-3-662-54823-3>.
51. Gogotsi, Y., Baek, C., & Kirscht, F. (1999). Raman microspectroscopy study of processing-induced phase transformations and residual stress in silicon. *Semiconductor Science and Technology*, 14(10), 936–944. <https://doi.org/10.1088/0268-1242/14/10/310>.
52. Yan, J., Asami, T., Harada, H., & Kuriyagawa, T. (2009). Fundamental investigation of subsurface damage in single crystalline silicon caused by diamond machining. *Precision Engineering*, 33(4), 378–386. <https://doi.org/10.1016/j.precisioneng.2008.10.008>.

Publisher's Note Springer Nature remains neutral with regard to jurisdictional claims in published maps and institutional affiliations.



Seyed Nader Ameli Kalkhoran received his B.Sc, M.Sc. and Ph.D from University of Mohaghegh Ardabili, Iran University of Science and Technology and K.N. Toosi University of Technology, Iran, in 2011, 2013 and 2020, respectively, all in Mechanical Engineering. His Ph.D. study was under the supervision of Dr. Vahdati since 2014. He was a visiting Ph.D. student at Keio University, Japan in 2018, under the supervision of Prof.

Yan. His research interests include molecular dynamics simulation and ultraprecision machining.



Mehrdad Vahdati received his Ph.D. in Mechanical Engineering from Utsunomiya University, Japan in 1996. At the moment, he is an associated professor at faculty of Mechanical Engineering, K.N. Toosi University of Technology. He is directing the laboratory of industrial machinery and the corresponding ongoing research projects in ultraprecision machining and magnetic field-assisted finishing and polishing processes.



Zhiyu Zhang is an associate research scientist of CIOMP (Changchun Institute of Optics Fine Mechanics and Physics Chinese Academy of Sciences). He received his bachelor's and master's degrees from Jilin University and doctorate from Tohoku University of Japan. His research interests include ultraprecision cutting/grinding and laser direct writing of diffraction optical elements. He has authored/co-authored more than 50 journal papers and 1 book chapter.



Jiwang Yan obtained his Ph.D. from Tohoku University, Japan in 2000 and is currently a professor of Mechanical Engineering at Keio University (2012-now), leading the Laboratory for Precision Machining and Nano Processing. His research areas include ultraprecision machining, micro manufacturing, nano-material processing, and nanomechanics. He has authored/co-authored 200+ peer-refereed journal papers and given 100+ keynote/invited talks. He has received 30+ awards for his contribution in the manufacturing area. He serves on editorial boards of 12 international journals.